CRYSTALLINE-TO-AMORPHOUS TRANSFORMATION OF INTERMETALLIC COMPOUNDS IN THE ZR-FE-M SYSTEM INDUCED BY IRRADIATION

Arthur T.Motta[1], Lawrence M. Howe[2] and Paul R. Okamoto[3]
1. Dept. of Nuclear Engineering, Pennsylvania State University, University Park, PA, 16802 USA.
2. AECL Research, Reactor Materials Research Branch, Chalk River Laboratories, Chalk River, Ontario, Canada, K0J 1J0.
3. Materials Science Division, Argonne National Laboratory, Argonne, IL 60439, USA.

ABSTRACT

The binary and ternary intermetallic compounds Zr_3Fe, Zr_2Fe, $(Zr_{0.5},Nb_{0.5})_3Fe$, $Zr_3(Fe_{0.9},Ni_{0.1})$ and $Zr_3(Fe_{0.5},Ni_{0.5})$ were subjected to 900 keV electron irradiation until amorphous to study the change in the dose-to-amorphization with temperature. The critical temperatures were observed to vary with dose rate, and with the type of compound. Hexagonal $(Zr_{0.5},Nb_{0.5})_3Fe$ had an appreciably lower critical temperature and higher dose to amorphization at low temperature than orthorombic Zr_3Fe, whereas other orthorombic $Zr_3(Fe_x,Ni_{1-x})$ compounds were essentially identical in behavior to Zr_3Fe. The electron energy dependence of the dose-to-amorphization was studied in Zr_3Fe between 250 and 900 keV. The analysis of the results gives displacement energies of $E_d^{Zr} = 26\,eV, E_d^{Fe} = 18\,eV$ in the Zr_3Fe compound.

INTRODUCTION

The crystalline-to-amorphous transformation (amorphization) of intermetallic compounds under irradiation has elicited great interest ever since it was first reported for the cases of neutron [1], ion [2] and electron [3] irradiation. Several reviews have been written describing the extensive experimental and theoretical work performed on the subject in the last decade [4-9]. Amorphization under irradiation occurs when a certain critical level of damage is surpassed [10]. At this critical level of damage accumulation, corresponding to a free energy increase in the irradiated crystalline phase which takes it above that of the amorphous phase, the irradiated crystalline phase becomes unstable with respect to the amorphous phase and amorphization can occur. There are several parameters that influence the amorphization process: the difference in free energy between the crystalline and amorphous phases (how much energy needs to be accumulated), the rate of damage production, the damage accumulation mechanisms in the intermetallic compound, and the annealing mechanisms available at the irradiation temperature.

By studying the kinetics of the amorphization process, it is possible to obtain information on those parameters. This paper reports two such studies we conducted in the Zr-Fe-M system. In the first study we investigated the amorphization kinetics of Zr_3Fe, Zr_2Fe, $(Zr,Nb)_3Fe$ and $Zr_3(Fe,Ni)$

during electron irradiation to determine the variation of the dose to amorphization with temperature, dose rate and ternary stoichiometry. In the second study we studied the change in dose to amorphization in Zr_3Fe with electron energy at low temperature and used the results to estimate displacement energies in both sublattices. We discuss the results in terms of existing amorphization models.

EXPERIMENTAL METHODS

Thin foil samples containing Zr_2Fe, $(Zr_{0.5},Nb_{0.5})_3Fe$ and $Zr_3(Fe_x,Ni_{1-x})$, with $x = 1, 0.9$ and 0.5 were prepared by arc melting and annealing, followed by mechanical polishing and electro polishing as described in [11]. The alloys were prepared off-stoichiometry to minimize handling problems due to brittleness. The result was a mixture of the desired phase and either Zr or Fe. Specific grains containing the phases desired were identified before irradiation by electron diffraction and energy dispersive x-ray analysis. Those were the grains later used in the irradiation. Electron diffraction and EDX analysis showed the Zr_2Fe phase was C16 bct [12]. The patterns from Zr_3Fe, $Zr_3(Fe_{0.9},Ni_{0.1})$ and $Zr_3(Fe_{0.5},Ni_{0.5})$ were indexed as orthorombic (o-Zr_3Fe) [13] . It was not possible to index the patterns from $(Zr_{0.5},Nb_{0.5})_3Fe$ as the orthorombic phase above, but they were all indexed as the hcp phase reported in [14] (h-$(Zr,Nb)_3Fe$).

Electron irradiations were performed in the Kratos HVEM Facility in the Electron Microscopy Center at Argonne National Laboratory. Two types of experiment were conducted. In the first type of experiment, (performed on $(Zr,Nb)_3Fe$, $Zr_3(Fe,Ni)$ and Zr_2Fe), the samples were irradiated at several temperatures with 900 keV electrons until they became amorphous. In the second type, samples of Zr_3Fe were irradiated at electron energies between 200 and 900 keV, at 25 K until they became amorphous. Careful beam dosimetry was performed in both cases. The effect of dose rate was investigated by measuring the amorphous radius as a function of electron dose using the Gaussian shape of the beam as in [11]. Pre- and post-irradiation examinations were conducted at Chalk River Laboratories using a Philips CM-30 electron microscope.

RESULTS

Figure 1 shows the electron dose to amorphization (in $electron.cm^{-2}$) versus irradiation temperature for Zr_3Fe, $Zr_3(Fe_{0.9},Ni_{0.1})$, $Zr_3(Fe_{0.5},Ni_{0.5})$, $(Zr_{0.5},Nb_{0.5})_3Fe$, and Zr_2Fe. It is important to define precisely the criterion for amorphization in order to obtain consistent results. The criterion for amorphization in this study was that the smallest diffraction aperture showed only an amorphous ring. Since the smallest diffraction aperture selects a 0.3 μm-diameter region, the dose plotted in fig. 1 is the dose necessary to form an amorphous region of 0.3 μm in diameter. In the case of the dose rate studies, there is a one-to-one correspondence between diameter and dose rate, e.g. a radius of 0.15 μm corresponds to a dose rate of 6×10^{19} $e/cm^2.s$, while at 1.5 μm the dose rate is 3.4×10^{19} $e/cm^2.s$. In this case, a sample is called amorphous when the diameter of the amorphous region corresponds to the dose rate desired.

The compound that is easiest to amorphize, having both the highest critical temperature and the lowest dose to amorphization is Zr_2Fe. This is followed by $Zr_3(Fe,Ni)$ and $(Zr_{0.5},Nb_{0.5})_3Fe$. The dose rate has a marked difference in the results for Zr_3Fe: as the dose rate changes from 6×10^{19} e/cm^2s (high dose rate case) to 3.4×10^{19} e/cm^2s (low dose rate case), the critical temperature of Zr_3Fe changes from 220 K to about 200 K. At 180 K, the dose to amorphization at 6×10^{19} e/cm^2s is five times smaller than that at 3.4×10^{19} e/cm^2s. Previously, in ^{40}Ar ion irradiations of Zr_3Fe, a pronounced dose rate effect was observed in the temperature range 160-280 K [15].
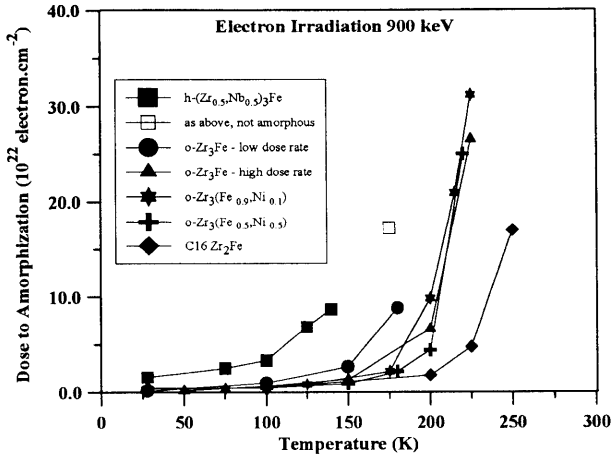

Figure 1: Dose to amorphization under electron irradiation as a function of .temperature for various compounds.
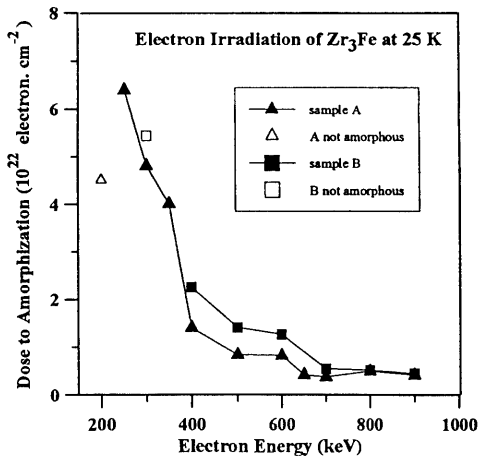

Figure 2: Dose to amorphization for Zr_3Fe at 25 K versus electron energy.

The effect of stoichiometry is less clear-cut. There is no difference observed in the critical temperatures of $Zr_3(Fe_x,Ni_{1-x})$, for $x = 1, 0.9$ or 0.5: they were all around 215 K. The dose to amorphization at low temperature was also the same for all three compounds. However there was a marked difference in the critical temperatures of o-Zr_3Fe (215 K) and h-$(Zr_{0.5},Nb_{0.5})_3Fe$ (150-160 K). The dose to amorphization of h-$(Zr_{0.5},Nb_{0.5})_3Fe$ at 25 K was 10 times higher than that of o-Zr_3Fe. That the crystal structure varies with stoichiometry in the Zr-Nb-Fe case and not in the Zr-Ni-Fe case could explain the different amorphization responses.

Figure 2 shows the change in the dose to amorphization of Zr_3Fe under electron irradiation at 23-30 K. The experiment was repeated in two different samples of Zr_3Fe (denoted A and B) with consistent results. Amorphization was achieved at electron energies as low as 250 keV. There are three different regions in the graph: from 900 to 700 keV, the dose to amorphization remains constant at about 5×10^{21} e.cm^{-2}; between 700 and 600 keV, it increases by a factor of two, again remaining constant between 600 and 400 keV, and increasing quickly between 400 and 250 keV. The difference in the dose for the two samples in the region below 600 keV is attributed to different impurity content, and is discussed in more detail below. Lastly, in the irradiations below 400 keV, preferential amorphization along particular crystalline directions was observed [16,17].

DISCUSSION

A model for amorphization under electron irradiation based on the elimination of mobile defects at the surface sink and the accumulation of the slow defect in the bulk of the material was presented in [18]. This model included point defect accumulation and chemical disordering (in the Bragg-Williams approximation) and explained both the effects of temperature and dose rate. The model, however, did not take into account the fact that the different defects that can exist in ordered intermetallic compounds (vacancies and interstitials in both sublattices and anti-site defects) may have different migration energies, as well as restricted (anisotropic) migration paths, as is the case for CuTi [19]. The quantitative modeling of the results shown in figure 1 would require as input the migration and formation energies of all the defects above for the compounds of interest.

In qualitative fashion, the annealing rate due to a particular defect increases with temperature as the defect becomes mobile, until at the critical temperature the annealing rate becomes higher than the damage rate, and no amorphization can occur. This means that the critical temperature for low-dose rate amorphization will be lower than for a high dose rate case. At low temperature annealing is not a factor and therefore there is no dose rate effect, as observed experimentally. Amorphization occurs when the dose-to-amorphization D is equal to the critical dose:

$$D = [G - v(T)]\, t = [\Phi\, \sigma_d - v(T)]\, t \geq D_{crit} \qquad (1)$$

where G is the dose rate, $v(T)$ is the annealing rate, t is the irradiation time, Φ is the electron flux, σ_d the displacement cross section, and D_{crit} is the critical dose for amorphization. Considering that at 25 K $v \cong 0$, then for each electron energy E at amorphization :

$$D(E) = \Phi \, t_{am}(E) \, \sigma_d = \Phi \, t_{am}(E) \sum_i x_i \, \sigma_d^i(E_d^i, E) = D_{crit} \qquad (2)$$

where x_i is the concentration of element i, σ_d^i its displacement cross section, E_d^i its displacement energy and t_{am} is the measured time to amorphization. Equation 2 states that when we multiply the values of the dose to amorphization as a function of energy given in figure 2 by the weighted displacement cross section (obtained from Oen's tables [20]), the result should be independent of energy. Since the values from Oen's tables are dependent on the displacement energy, it is possible to find the set of displacement energies that best fits the experimental data. As explained in [16,21] displacements can also occur by a secondary displacement mechanism, mediated by light element impurities [21]. The impurity concentration was measured with the forward elastic recoil detection technique, and found to be 1-3% oxygen [22]. If the impurity is oxygen, then :

$$D(E) = \Phi \, t_{am}(E) \, [\,0.75\, \sigma_d^{Zr} \,(E_d^{Zr}, E) + 0.25\, \sigma_d^{Fe}\,(E_d^{Fe}, E) + x_O \, \sigma_d^{O}\,(E_d^{O}, E)\vartheta_O^{Zr,Fe}\,] = D_{crit}. \qquad (3)$$

where $\vartheta_O^{Zr,Fe}$ is the number of displacements in the Zr, Fe lattices caused by each O displacement ($\vartheta_O^{Zr,Fe}$ was taken to be 1). Using the value of 3% impurity concentration for sample A, equation 3 was used to fit the data by minimizing the least squares deviation from the horizontal. The fit was optimized for sample A data, and the same values used for sample B, changing only the impurity content. Since sample B had a higher value of the dose-to-amorphization at lower energies, a lower impurity content (1%) was used. The fit is shown in figure 3, and explains the results well, for the set of values $E_d^{Zr} = 26\,eV$, $E_d^{Fe} = 18\,eV$, $E_d^{O} = 12\,eV$.
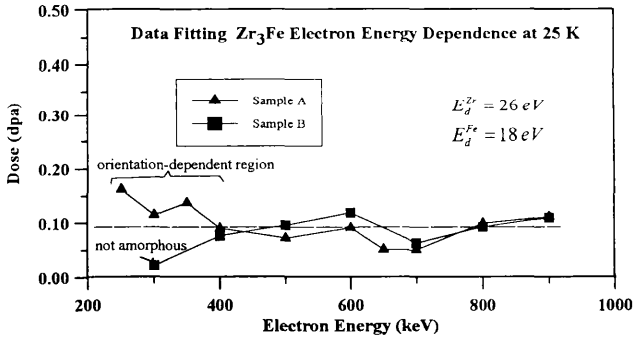

Figure 3: The optimized profile of dose to amorphization versus electron energy.

CONCLUSIONS

1. The critical temperature for amorphization of h-$(Zr_{0.5},Nb_{0.5})_3Fe$ was found to be 30 to 60 K lower than that of o-Zr_3Fe. The dose to amorphization of h-$(Zr_{0.5},Nb_{0.5})_3Fe$ was 10 times smaller than that of o-Zr_3Fe at 25 K. No difference was found in either the critical temperatures or the dose to amorphization at 25 K of o-Zr_3Fe, o-$Zr_3(Fe_{0.9},Ni_{0.1})$ and o-$Zr_3(Fe_{0.5},Ni_{0.5})$.

2. The critical temperature for amorphization of o-Zr_3Fe increases with dose rate: increasing the dose rate by a factor of two caused a 20 K increase in the critical temperature.

3. The critical temperature of Zr_2Fe is about 250 K.

4. By fitting the data obtained for the dose-to-amorphization of Zr_3Fe, the displacement energies in the individual sublattices are estimated to be $E_d^{Zr} = 28\,eV$ and $E_d^{Fe} = 18\,eV$.

ACKNOWLEDGMENTS

REFERENCES

1. J. Bloch, Journal of Nuclear Materials, 6 (1962) 203
2. L. M. Howe and M. Rainville, Phil. Mag. A 39(2) (1979) 195-212.
3. G. Thomas, H. Mori, H. Fujita and R. Sinclair, Scripta Met. 16 (1982) 589-592.
4.. C.Jaouen, Solid State Phenomena 23&24 (1992), 123-146.
5. P. R. Okamoto and M. Meshii, in Science of Advanced Materials eds. H. Wiedersich and M. Meshii (ASM, 1992), 33-98.
6. M. Nastasi and J. W. Mayer, Materials Science Reports 6 (1991) 1.
7. A. T. Motta and C. Lemaignan, in "Ordering and Disordering in Alloys" ed. A. R. Yavari, Elsevier, 1992, 255-276.
8. D. F. Pedraza, Met. Trans. A Vol. 21A (1990) 1809-1815.
9. L.M.Howe, in "Intermetallic Compounds: Principle and Practice", eds. J.H.Westbrook and R.L.Fleischer, John Wiley and Sons, 1994, in press.
10. L. M. Howe and M. Rainville, Journal of Nuclear Materials, 68 (1977) 215-234.
11. A.T.Motta, L.M.Howe and P.R.Okamoto, J. of Nucl. Materials, 205 (1993) 258-266.
12. E.E.Havinga, H.Damsma and P.Hokkeling, J.Less-Comm. Metals, 27(1972) 169-186.
13. F.Aubertin, U.Gonser, S.J.Campbell, and H.-G.Wagner, Z.Metallk. 76 (1985) 237.
14. O.T.Woo and G.Carpenter, Proc.12th Int.Congr. El. Micr., 1990, San Francisco Press, 132.
15. L.M.Howe, M.H.Rainville and D.Philips, MRS Symp.Proc 236 (1993) 461.
16. A.T.Motta, L.M.Howe and P.R.Okamoto, MRS Symp.Proc.316 (1994) 265-270.
17. L.M.Howe, D.Philips, A.T.Motta, and P.R.Okamoto, Surf. Coat. and Tech.,66 (1994) 411.
18. A. T. Motta and D. R. Olander, Acta Metall.et Materialia, 38(11) (1990), 2175-2185.
19. J.R.Shoemaker, et al., J.Mat.Res. 6(3) (1991), .473-482.
20. O.S.Oen. ORNL report 4897, 1973.
21. P.G.Regnier, N.Q.Lam and K.H.Westmacott, J.Nucl.Mater., 115 (1983) 286
22. L.M.Howe, J.S.Forster, R.Siegele and J.A.Davies, to be published.